Coastal Engineering 56 (2009) 59–72

Contents lists available at ScienceDirect

Coastal Engineering

journal homepage: www.elsevier.com/locate/coastaleng

Modeling the erosion of cohesive clay coasts

Alan S. Trenhaile *

Department of Earth Sciences, University of Windsor, Ontario, Canada N9B 3P4

ARTICLE INFO

Article history:
Received 5 February 2008
Received in revised form 5 May 2008
Accepted 3 July 2008
Available online 9 August 2008

Keywords:
Cohesive coast
Soft rock
Model
Waves
Tides

ABSTRACT

A model was developed to study the erosion of cohesive clay coasts in macro- to non-tidal environments. The model shares some of the characteristics of previous models, including the erosion of bare clay surfaces by wave generated bottom shear stresses, and of mobile, sediment-covered surfaces by abrasion. It differs from previous models, however, in several important ways. The morphodynamics of beaches with clay foundations, under different wave conditions, are based on a previously developed model for beaches on rocky shore platforms. Sediment thickness along a beach profile is calculated at regular intervals and compared with the maximum thickness that could be moved at that location under prevailing wave conditions. Wave friction factors are determined, where necessary, according to the occurrence and morphology of ripples on the bottom. In addition to abrasion and the effect of wave induced shear stresses on the clay bottom, erosion by stresses generated by wave impact at the bluff foot and on the intertidal platform is calculated using an expression derived from hard rock coastal models. Tides are represented by their computed tidal duration values, the amount of time each year that the water level falls within each 0.1 m vertical interval. Water depths are modified by wave setup and set-down conditions. Several preliminary model runs were made. The profiles were concave in the submarine zone and roughly linear in the intertidal zone. Equilibrium profiles developed which were maintained as they migrated landwards.

1. Introduction

Cohesive coasts develop in materials with high clay content. These coasts often consist of a steep, and sometimes gullied, bluff behind a clay shore platform which may be covered, wholly or in part, by a thin sand or gravel beach. The erosional resistance of a cohesive material is complex, depending on the nature and strength of the intergranular forces, mineralogy, and the physiochemical environment, and it is a function of its compressive or shear strength, clay content, plasticity, consolidation pressure, clay structure, and the properties of the pore water and eroding fluid (Kamphuis, 1987; CEM, 2002).

Most work on the erosion of cohesive clay coasts has been conducted by engineers, whereas most work on rocky coasts has been by geomorphologists and geologists. Engineers are interested in clay coasts because of their rapidly changing and eroding nature and the consequent risk to human structures and activities; conversely, remote or slowly eroding hard rock coasts generally pose little threat to human safety. For much the same reasons, coastal engineers are also concerned with sandy beach morphology and dynamics and, despite quite different erosional processes, engineering designs, research, and most textbooks have treated sandy and cohesive clay coasts as being essentially the same, with only minor differences (Kamphuis, 1986). This is reflected in comparisons that have been made between cohesive clay and sandy coasts (Philpott, 1984; Kamphuis, 1990) rather than, more appropriately, between cohesive clay and rock coasts.

Although clay coasts change more rapidly than most rocky coasts, they share the fundamental characteristic, which distinguishes them from beaches, that erosion and coastal retreat are irreversible. The traditional distinction that has been made between clay and rock coasts is untenable, and it has discouraged the exchange of mutually beneficial ideas. Clay coast researchers are generally unfamiliar with relevant geomorphological work on rock coasts. For example, it has been a basic tenet of conceptual rock coast modeling for almost a century, and of numerical modeling for more than 40 years, that because of the relationship between rates of wave attenuation and bottom depths and gradients, cliff retreat is ultimately controlled by erosion of the inter- and subtidal shore platform (e.g. Johnson, 1919; Flemming, 1965). It is only fairly recently, however, that this concept, derived independently, has found its way into the cohesive clay coast literature (Philpott, 1984; Davidson-Arnott, 1986; Bishop et al. 1992; Davidson-Arnott and Ollerhead, 1995).

Rock coasts vary enormously in morphology and in the erosional efficacy of the processes that operate on them; consolidated, cohesive clay coasts represent a 'soft rock' subset of this broad spectrum of processes and forms. Wave erosional efficacy and the nature of the dominant processes on rocky coasts vary in space and time, according to surface gradient and roughness, and particularly as to whether

* Tel.: +1 519 253 3000x2184; fax: +1 519 973 7081.
E-mail address: tren@uwindsor.ca.

0378-3839/$ – see front matter © 2008 Elsevier B.V. All rights reserved.
doi:10.1016/j.coastaleng.2008.07.001

high, seaward facing scarps or upstanding beds of dipping rock promote water hammer and air compression in joints, bedding planes and other discontinuities (Fig. 1). Weathering efficacy also varies from one rock type to another, depending on its physical and chemical characteristics, and from place to place according to the prevailing climate and the elevation of the site with respect to the tides (Trenhaile, 1987). As on some other rock coasts, wave quarrying on clay coasts is inhibited by the occurrence of generally smooth, gently sloping intertidal surfaces, and the dominant processes at elevations below the bluff foot are usually abrasion, where there is suitable loose material, and downwearing by granular breakdown owing to weathering and to shear stresses generated by turbulence and hydrostatic variations in pressure beneath shoaling waves and surf (Coakley et al. 1986; Bishop et al., 1992; Skafel and Bishop, 1994; Skafel, 1995).

The present paper discusses the structure of a model that has been developed to study the erosion of cohesive clay coasts. Although this model shares some of the characteristics of previous clay coast models (Nairn et al. 1986; Kamphuis, 1986, 1987; Healy et al., 1987; Walkden and Hall, 2005) there are significant differences, some of which are derived from the author's experience with modeling the erosion of hard rock coasts (Trenhaile, 2000, 2001, 2005). The terms 'bluff' and 'cliff' are used in this paper to refer to steep coastal slopes in clay (soft rock) and rock (hard rock), respectively.

2. The model

The model is two-dimensional. Shore-normal profile retreat and development are determined using expressions that calculate the amount of erosion by wave induced bottom shear stresses and wave abrasion in the subtidal and intertidal zones, and by stresses generated by surf impact in the intertidal zone and at the foot of bluffs. S.I. units are used throughout this discussion.

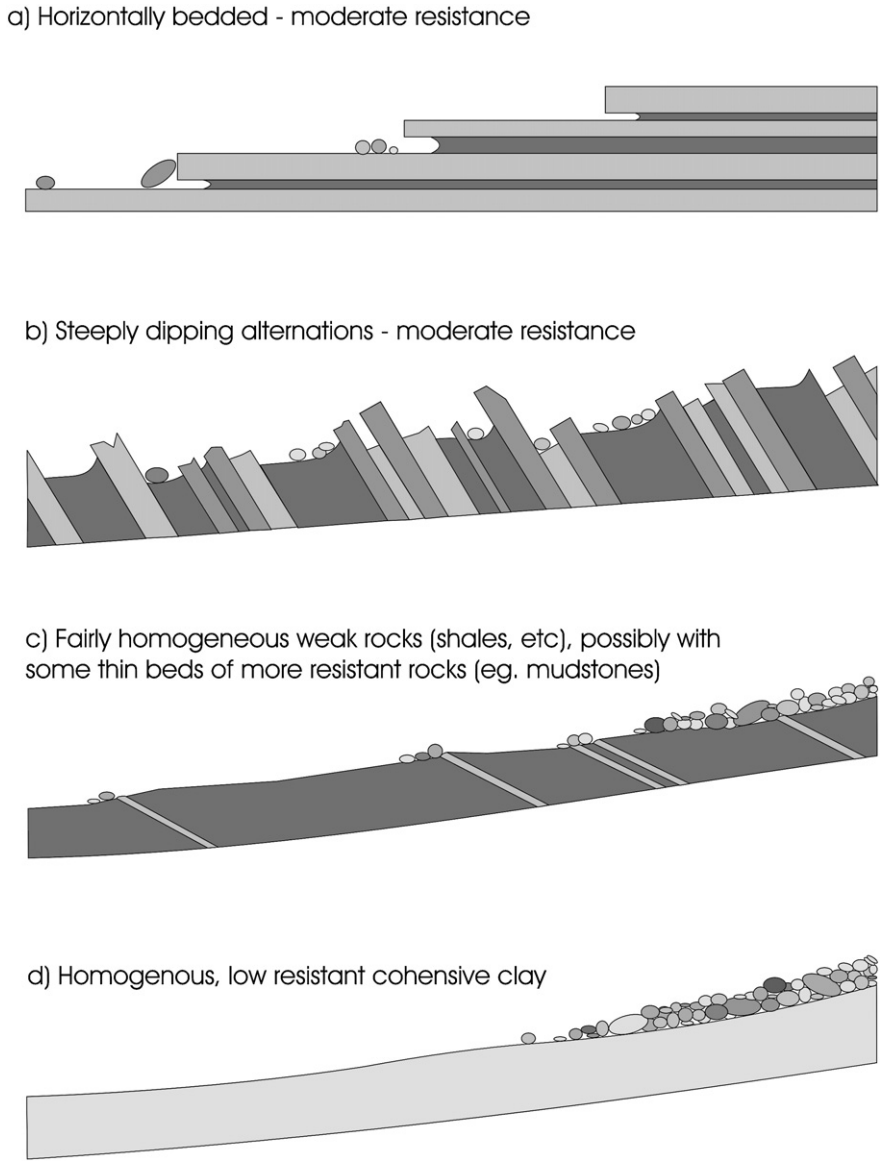

Fig. 1. Some types of rock coast. a) and b) are dominated by wave quarrying by wave impact and air compression in structural discontinuities (joints, bedding planes) at, or close to the water surface. Abrasion may occur between, or at the foot of rock structures. Weathering plays a secondary role and wave induced bottom shear stresses are too low to erode the rock, although they may help to remove weathered material. c) Wave quarrying is inhibited by the lack of steep structures. Weathering (wetting and drying, etc) dominates, especially in argillaceous rocks, and abrasion is important where there are suitable materials. Bottom shear stresses cannot erode unweathered rock but they can assist in the dislodgement and removal of weathered material. d) is similar to c) although in addition to abrasion, bottom shear stresses may be sufficient to erode the clay.

2.1. Waves

Waves can be inputted into the model as a time series or as a discrete number of waves sampled from a distribution. As waves begin to shoal, changing wave height in transitional and shallow water, defined as being where $0.25>h/L_o>0.05$ and $h/L_o<0.05$, respectively, where h is the water depth and L_o is deep water wavelength, can be represented by:

$$H = H_o\sqrt{(C_o/2Cn)} \tag{1}$$

where H and H_o are wave height in intermediate/shallow and deep water, respectively. Linear (Airy) wave equations are used to determine C_o, the deep water wave celerity, and Cn, the group wave celerity in intermediate and shallow water. Wavelength in shallow water was determined using linear wave theory, and in intermediate depths using the CEM (2002) equation:

$$L = L_o\sqrt{[\tanh(2\pi h/L_o)]} \tag{2}$$

where L is the wavelength in intermediate or shallow water.

There is no wave orbital velocity at the bed in deep water ($h/L_o>0.25$). According to linear wave theory, the maximum bottom orbital velocity (u_o) in intermediate depths can be represented by:

$$u_o = \pi H/(T\sinh kh) \tag{3}$$

and in shallow water by :

$$u_o = (H/2)\sqrt{(g/h)} \tag{4}$$

where T is the wave period, g is the acceleration due to gravity, and k is the wave number ($2\pi/L$).

The shear stress exerted on the bottom by the waves (τ) is given by:

$$\tau = 0.5\, F_w\, \rho u_o^2 \tag{5}$$

where F_w is the friction factor and ρ is the density of sea water (1030 kg m^{-3}). Friction factors are calculated in the model using Justensen's (1988) data, based on the value of A_b/k_s, where A_b is the amplitude or half the length of the horizontal water motion at the bottom (determined for intermediate and shallow water using linear wave theory), and k_s is the Nikuradse roughness length for a rippled bed or the equivalent roughness length for a plane bed.

Although many workers proposed that breaker depth is determined by such factors as wave period and steepness, bed slope, and the surf similarity parameter, Balsillie and Tanner (2000) demonstrated that it is almost entirely related to wave height, according to the expression, which was derived more than a century ago:

$$\gamma_b = H_b/h_b = 0.78 \tag{6}$$

where γ_b is the breaker depth index, h_b is the depth of wave breaking and H_b is the mean breaker height. The depth of the breaker and the gradient of the bottom are used in the model to calculate the width of the surf zone. Wave height in the surf zone is calculated using Sunamura's (1985) expression:

$$H = H_b\exp\left\{[-35.2D_b\tan\beta]\Big/\left[T\sqrt{(gh_b)}\right]\right\} \tag{7}$$

where β is the slope of the surf zone and D_b is the distance shorewards from the breakers.

There is no acceptable theory to describe complex water movement in the surf zone. Several workers have used the rate of energy dissipation, represented by the rate of wave height decay, as indicative of spatial and temporal erosional patterns (Kamphuis, 1986, 1987; Nairn et al., 1986; Walkden and Hall, 2005); as bottom shear stresses provide the erosional mechanism, this approach associates surf zone shear stresses with changes in the height of the waves (i.e. with dH/dD_b). Whereas surf zone energy dissipation rates can be related to changes in wave height, however, their erosional effect on the bottom is likely to increase with the height of the waves and to decrease with the depth of the water, such that shear stresses on the bottom would then be a function of the term $(H/h)(dH/dD_b)$. Alternatively, as bottom shear stresses in the surf zone are dominated by oscillatory flow (Coffey and Nielsen, 1984; Diegaard et al., 1986), they might be approximated using Eqs. (4) and (5), which suggest that shear stresses are related to the term H^2/h. The three approximations were compared to determine how they represent changes in bottom shear stresses, and consequently wave erosion, across the surf zone (Fig. 2). The trends shown by the three variables are similar, with their highest values occurring in the outer region near the breakers; the absolute shear stress values would depend on the coefficients used in each equation, as, for example, in the equation relating surf shear stresses to changes in the height of the waves.

The occurrence of similar spatial trends suggests that any of the three variables can provide suitable representations for shear stress or bottom erosion calculations in the surf zone. It was decided, however, to use the same methodology, which is based on the H^2/h term, to approximate bottom shear stresses and erosion in the surf zone as in the shallow water outside the breakers. The advantage in using this approximation is that only one constant is required to relate erosion rates to wave conditions inside and outside the breaker zone, rather than the two that would be needed using shear stresses outside the breaker zone and energy dissipation rates inside the surf zone. Although it has been proposed that decreasing wave height and orbital velocity in the surf zone is inconsistent with the inverse relationship between depth and the erosional driving forces, and consequently with an increase in erosion towards the shoreline (CEM, 2002), field data are lacking to support this contention. The parallel clay slope retreat model (Philpott, 1984), which was devised for non-tidal bodies of water, suggests that rates of erosion must be greatest in the more steeply sloping portions of the subaqueous profile near the shore, but these areas are generally covered in beach material and subjected to abrasion rather than to wave generated bottom shear stresses.

The type of breaking wave affects rates of energy dissipation and rates of wave height decline in the surf zone, and therefore also the rate at which wave generated shear stresses decrease from the breakers to the shoreline. Energy is dissipated more rapidly by plunging than by spilling breakers. Trenhaile (2000) used the Iribarren Number, the breaker equivalent of the Surf Similarity Parameter (Battjes, 1974) to determine the type of breaker (based on deep water wavelength, breaker height, and bottom slope) and to account for known differences in the forces that they generate in the surf zone. The Surf Similarity Parameter was also used by Kamphuis (1986) as a measure of the rate of energy dissipation in the surf zone. Sunamura's (1985) expression (Eq. (7)) for wave height in the surf zone was derived from different types of coastal environment, including Japanese and Barbados field data and from a very large wave tank; his expression therefore represents the mean of a wide variety of breaker types. For this reason, and because we lack precise data on the relationship between breaker type and patterns of energy dissipation or bottom shear stresses in the surf zone, the effect of different types of breaker is not considered in the present study.

The stresses generated by wave breaking causes water to pile up against the shore, thereby elevating the mean water level in the surf zone (wave setup). A corresponding depression of the water surface (set-down) occurs at, and offshore of the breakers. Wave setup and set-down, through changes in the depth of the water, affect such factors as the wavelengths, bottom orbital velocities and amplitudes of the waves and the bottom shear stresses that they generate. They are

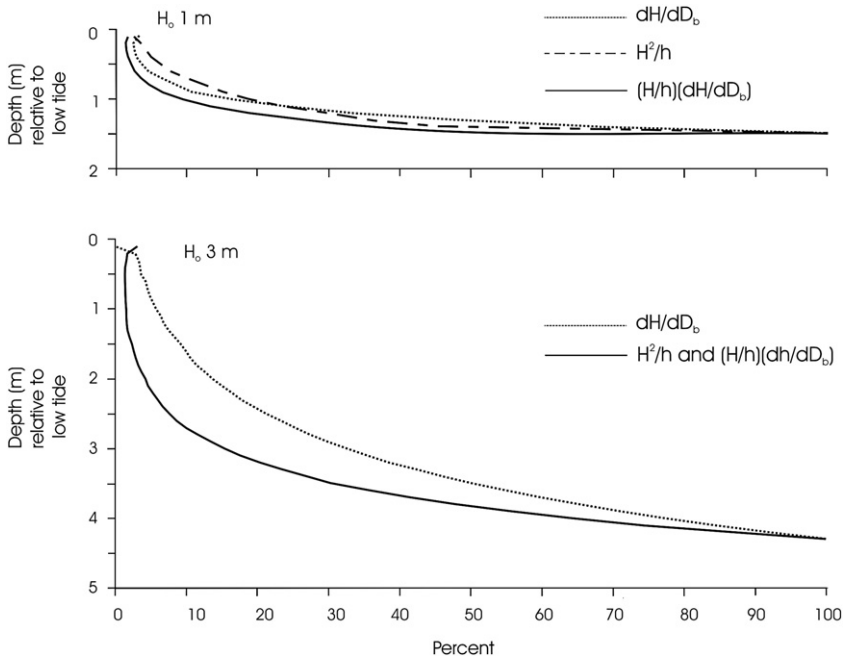

Fig. 2. Shoreward changes in three wave variables in a surf zone with a linear bottom (β=2°) for waves with 1 m and 3 m deep water wave heights. Values are expressed as percentages of the value of each variable at the first elevational interval shorewards of the breakpoint. The change in wave height at a particular elevational level (dH/dD_b) was calculated according to the height of the shoaling wave at the level immediately below and above that level (i.e. ±0.1 m).

incorporated in the model using the CEM (2002) equations for set-down:

$$\eta = -\pi H^2/[4L\sinh(2kh)] \tag{8}$$

and for setup

$$d\eta/dx = \tan\beta/\left[1 + (8/3\gamma_b^2)\right] \tag{9}$$

where η is the mean water surface elevation relative to the still water level and dη/dx is the gradient of the water surface in the surf zone.

2.2. Tides

Small tidal prisms in the shallow waters of open ocean coasts are unlikely to exert bottom stresses that are high enough to erode consolidated clays, and the clay coasts of the lower Great Lakes are in essentially non-tidal environments. Much larger tidal prisms and stronger currents can be generated in macrotidal estuaries, including the Bay of Fundy in eastern Canada, where maximum bottom current velocity is about 2 m s^{-1} (Dalrymple et al., 1990). The clays that are exposed to these strong, generally longshore, tidal currents generally settled from suspension onto mudflats, however, and the surface materials are unconsolidated and experience cycles of both erosion and deposition.

Although tides probably do not contribute directly to the erosion of clay coasts, they play an important role in directing the work of the waves. The focus of wave erosion, whether by shear stresses, abrasion, or wave impact stresses, moves up and down the inter- and subtidal zones with the ebb and flow of the tides. Waves operate at some tidal levels more frequently and for longer durations than at others. Tidal elevation, the duration of the slack periods at the low and high tidal levels, and rates of water surface migration at intermediate elevations are determined by the tidal range, which varies from one tide to the next in a complex manner according to changes in the distance and declination of the tide-generating bodies. Sandy beaches can quickly adjust to prevailing tidal conditions, but cohesive coasts change more slowly and their erosion and morphology reflect longer term variations in the time that the water surface occupies different elevations within the intertidal zone (Trenhaile, 2000, 2001).

Tidal duration distributions describe the absolute (h yr^{-1}) or proportional (%) amount of time that the surface of the water is within a given range of elevations in the intertidal zone (Trenhaile, 1987). For the present study, Smart and Hale's (1987) program was used to obtain tidal duration data from eastern Canada, for macrotidal St. John in the Bay of Fundy and for meso- to microtidal Mont Louis in Gaspé, Québec (Fig. 3). Tidal data were obtained for each port from published tide tables (Fisheries and Oceans Canada, 2006). The analysis showed that the water level is most frequently at, or close to, the neap high and

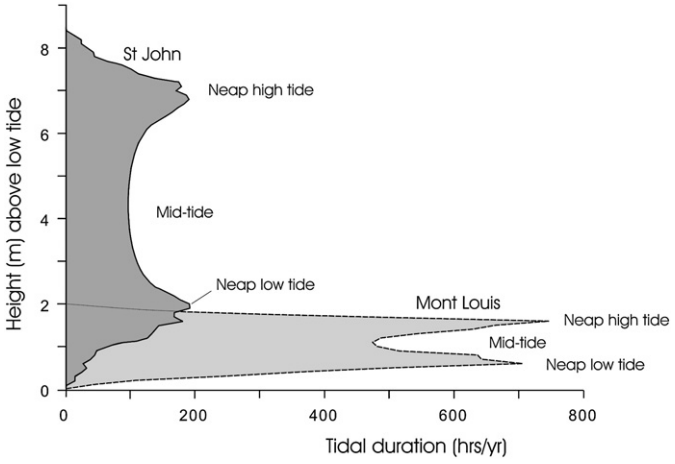

Fig. 3. Tidal duration distributions for two ports in eastern Canada. Duration values were calculated to represent the time that the water surface is within each 0.1 m vertical interval. There are 20 intervals and 21 tidal duration values for Mont Louis, Québec (2 m tidal range) and 83 intervals and 84 tidal duration values for St John, New Brunswick (tidal range 8.3 m tidal range). The total duration value, the sum of each of the 0.1 intervals, is equal to the number of hours in a year. For a non-tidal body of water, as in the Great Lakes, the tidal duration value is for only one vertical interval, and is equal to the number of hours in a year.

low tidal levels. The frequency, or duration, decreases by about one-third to one-quarter to the mid-tidal level, and it declines very rapidly from the neap to the spring high and low tidal levels. The duration values at each intertidal elevation are much higher in low than in high tidal range environments.

2.3. Beach material

Although eroded fine-grained sediment is generally carried offshore, glacial tills often contain some sand and gravel, and beach material can also be obtained from associated glacio-fluvial deposits, and from river and other coarse sediment transported alongshore. Coarse-grained sediments on inter- and subtidal clay surfaces (shore platforms) are swept back and fore by the waves, facilitating abrasion of the underlying clay. The base of thick deposits can be immobile, however, and act to protect the underlying surface from erosion (Robinson, 1977a). Therefore, abrasion rates under beach sediments are determined, in part, by fluctuations in the thickness and width of the deposits, which help to determine the spatial and temporal accessibility of the underlying clay to wave action.

Beaches are usually able to adjust fairly quickly to changing wave conditions (Wright and Short, 1984; Short, 1999), but rapid changes are more difficult for foreshore and nearshore zones that consist of beaches with clay foundations. There has been little attempt to study the occurrence and morphodynamics of beaches with resistant foundations in the field, but Trenhaile (2004) modeled their development and dynamics on rocky shore platforms, and that model is used in the present study to predict the thickness of beach sediments over clay surfaces under variable wave and tidal conditions. Although there have been many attempts to predict beachface gradient, Sunamura's (1989) empirical expression is used in this model because it was derived from the analysis of published field data from a variety of coastal environments:

$$\alpha = \tan^{-1}\left\{0.12/\left[H_b/\left(g^{0.5}D^{0.5}T\right)\right]^{0.5}\right\} \quad (10)$$

where α is beachface gradient and D is the sediment grain size. Therefore, according to Eq. (10), and consistent with the field evidence, beach deposits become thinner and more gently sloping during storms, and they extend further seawards.

It is assumed in the model that because coarse material is transported landwards, the beach extends seawards from the bluff for a distance determined by the amount of material and the slope of the beachface; these factors also determine the occurrence and width of the horizontal terrace, or berm, at the foot of the bluff. Depending on the gradient of each section of the underlying clay platform, the beach could be a single, contiguous deposit or it could consist of two or more deposits separated by upstanding clay outcrops. Lacking an adequate theory for their occurrence, the model did not consider the presence of isolated patches of sediment at variable distances offshore, or the effect of submarine bars (Davidson-Arnott and Langham, 2000).

The model first determines whether a beach is able to extend from the foot of the bluff down to a given tidal level under prevailing wave conditions. This calculation is based on a comparison between the inputted amount of available sediment and the amount required to form a beach with the required gradient (Eq. (10)). If there is not enough sediment then beach thickness for that wave at that tidal level is zero. Conversely, if there is more than enough sediment for a beach to extend to that tidal level, the calculations are repeated below the tidal level, increasing in depth in 0.1 m increments, until the point is reached where there is not enough sediment for a beach. Beach sediment thickness (ζ_t) is then determined for each elevational increment extending from the bluff to the foot of the widest beach that can develop (Fig. 4).

Abrasion is possible only if the abrasives can be moved over the underlying surface; a deposit that is too thick protects the underlying material. There have been several attempts to determine the thickness of the moving sediment layer. Estimates have usually been from 0 to about 0.25 m, but they have ranged up to more than 0.5 m. The model uses Sunamura and Kraus's (1985) methodology, which relates the thickness of the mobile sediment layer to the Shields Parameter (Θ):

$$\Theta = 0.5F_w\rho u_o^2/[(\rho_s-\rho)gD] \quad (11)$$

where ρ_s is the density of the sediment (2650 kg m^{-3} for quartz). The thickness of the moving layer is a function of the excess Shields parameter:

$$\zeta_{t\max} = 81.4D(\Theta_b-\Theta_{cr}) \quad (12)$$

where $\zeta_{t\max}$ is the maximum thickness of the moving layer, Θ_b is the Shields Parameter at the breakpoint, and Θ_{cr} is the critical or threshold Shield Parameter for the onset of grain movement. According to Madsen and Grant (1976), Θ_{cr} is between 0.03 and 0.05 for quartz sand between 0.2 and 2 mm in diameter; a value of 0.04 is used in the model runs.

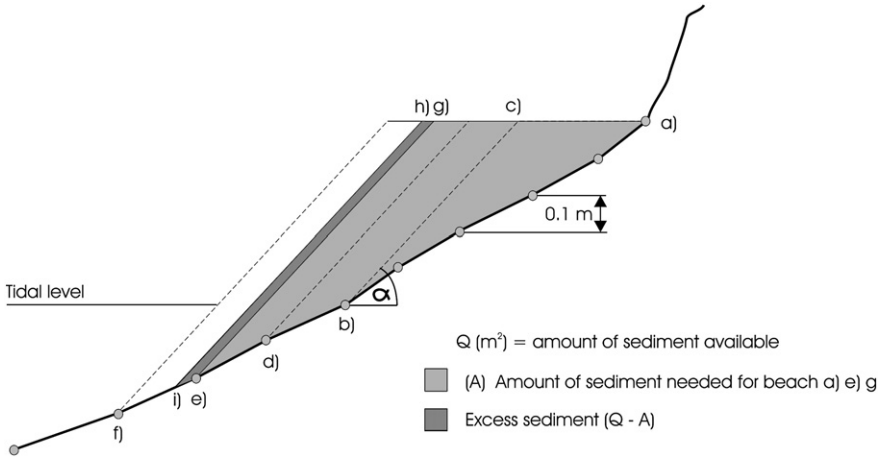

Fig. 4. Calculating beach occurrence and extent for a given wave and tidal level. It is first determined whether the amount of beach material specified in the model run is sufficient to form the beach with its foot at a specific tidal level for a given wave (b)). If not, then no beach material can extend to that tidal level and beach thickness at that elevation is zero for the given wave conditions. If there is enough sediment for a beach to extend to at least the tidal level, the calculations are repeated, for increasingly greater depths below the tidal level (d), e), etc.) until there is not enough sediment to form the beach (in this case, with its base at f)). The morphology of the beach (in this case, a), h), and i)) is determined according to the amount of sediment available in excess of the amount required for a beach to extend at its base to station e). Beach sediment thickness (ζ_t) is then determined at each tidal level geometrically. This series of calculations is repeated for each tidal level (at 0.1 m intervals) between the extreme low and high tidal levels for each model year.

Use of the Shields Parameter to determine the depth of the mobile layer requires friction factors for the surface of sand and other loose sediments, which may have ripples or other bedforms. There have been many attempts to predict the occurrence and morphology of ripples under specified conditions (Wiberg and Harris, 1994; Traykovski, 1999). The present study uses the relationships that have been established recently by O'Donoghue et al. (2006):

$$R_\eta = A_b\left(0.275{-}0.022\psi^{0.42}\right) \tag{13}$$

$$R_\lambda = A_b\left(1.97{-}0.44\psi^{0.21}\right) \tag{14}$$

where R_η is ripple height, R_λ is ripple wavelength, and ψ is the Mobility Number, a modified form of the Shields Parameter which is based on velocity rather than shear stress:

$$\psi = \rho u_o^2/[(\rho_s{-}\rho)gD] \tag{15}$$

There have been several attempts to represent the contribution of ripples to the relative bed roughness (Vongvisessomjai, 1984; van Rijn, 1989). The effect of ripples is represented in the model by (Nielsen, 1992):

$$k_s = \left(8R_\eta^2/R_\lambda\right) + 2.5DF_w\psi \tag{16}$$

where F_w is the grain roughness friction factor for a flat bed of sand. The friction factor on a rippled bed (based on the ratio A_b/k_s) is then used in Eq. (11) to determine the maximum depth of the moving sediment layer. If the local Shields Parameter is equal or greater than 1, no ripples develop and the Nikuradse Roughness Length on a flat bed of sand or gravel can be represented by Engelund and Hansen's (1967) expression, which was recommended by Sleath (1984):

$$k_s = 2D \tag{17}$$

(although Engelund–Hansen actually used D_{65}, where the subscript refers to grain diameter coarser than 65% of the sample, diameter is represented in the present study by a single value, rather than by a distribution of grain diameters). This value is then used (as A_b/k_s) to determine the friction factor in Eq. (11) for a flat sediment surface with no ripples.

2.4. Erosion

There is continuing debate over the erosive efficacy of wave induced shear stresses and abrasion on cohesive clay coasts (CEM, 2002). Coakley et al. (1986) found that bottom shear stresses in western Lake Ontario, computed from hindcast wave data, exceeded the critical stress for about 61 h/yr. Although they concluded that shear stresses may be a very important cause of subaqueous erosion, others proposed that erosion cannot occur in the absence of abrasive material. Kamphuis (1990) found that till on the north shore of Lake Erie is generally much too strong to be eroded by wave generated shear stresses alone, although much lower shear stresses can initiate erosion where granular abrasives are present. This conclusion was supported by Bishop et al. (1992), who reported that little or no erosion occurred in the absence of sand in an experimental study using intact blocks of cohesive till from the northern coast of Lake Erie. These conclusions are not consistent, however, with observations that the erosion of sand-free areas under plunging breakers, where turbulent jets are directed down to the bottom, can be similar, or even higher, than in sandy areas within the surf zone (Skafel and Bishop 1994, Skafel 1995).

Davidson-Arnott and Ollerhead (1995) used a modified micro-erosion meter to measure subaqueous erosion rates in the over-consolidated tills of western Lake Ontario. They found that rates range from more than 30 mm yr^{-1} at depths of less than 3 m, to less than 15 mm yr^{-1} at depths of more than 6 m. Abrasives are largely restricted to shallow water in this area, and wave generated bottom shear stresses are generally too low to account for the erosion of unaltered clay at depths of several metres. The authors concluded that erosion might be related to the gradual softening of the clay surface by cyclical loading and unloading associated with the oscillatory nature of the wave generated stresses. As most softening occurs within a few days on newly exposed surfaces (Davidson-Arnott, and Langham, 2000), the process is most effective where there is fairly rapid erosion and removal of the weakened surface material by bottom shear stresses and abrasion. This suggests that the effect of softening in reducing surface strength can be represented in cohesive clay models by decreasing the strength (critical shear stress) of the clay uniformly along the profile. Softening will then be most effective in shallow water, where softened surface layers can be most rapidly removed and renewed.

Clay strength on exposed tidal flats can be increased through evaporation (Amos et al., 1992) or reduced by wetting and drying, freezing and thawing and other subaerial weathering processes. The breakdown of clay-rich rocks by wetting and drying and salt weathering is most effective in the upper interidal zone, which has the longest periods of exposure and drying (Kanyaya and Trenhaile, 2005; Trenhaile, 2006, Trenhaile et al. 2006). No data are available on subaerial weathering rates in the intertidal zones of cohesive clay coasts. Therefore, although the relationship between elevation and rates of breakdown may be similar in cohesive clays to that in hard, argillaceous rocks, consideration of the effect of weathering in the model would require further assumptions and unknown coefficients, which could not be justified at present.

Erosion rates for bare clay surfaces are determined in the model according to bottom shear stresses below the water surface and stresses generated by wave impact at the water surface, and for surfaces covered by sediment by abrasion efficacy. The model determines whether there is any beach material at a particular elevation at, or below, the tidal level, for each type of wave (Fig. 4). If there is no sediment, then erosion is only possible as a result of water impact stresses and shear stresses at and below the water surface, respectively. If sediment is present, then the program compares sediment thickness with the maximum thickness that could be moved at that point. If the deposit is thicker than the maximum, then no movement can take place at the clay-sediment interface, and the sediment protects the underlying clay from erosion by shear stresses, wave impact stresses, and abrasion. If the thickness of the sediment is less than the maximum, then abrasion of the underlying clay can take place.

Clay erosion rates have been calculated in different ways. Kamphuis (1987) developed an expression for the erosion rate based on wave height and period, bottom slope, and a coefficient related to the strength of the material and some hydrodynamic constants; this expression was used in Walkden and Hall's model (2005). Many sediment erosion and transportation equations are based on the relationship between ambient and threshold conditions (air or water velocity, shear stress, Shields Parameter, etc) (Watanabe et al., 1980; Vincent et al. 1981; Williams et al. 1989) and this approach has been used to model the erosion of rock coasts (Trenhaile, 2000). Several workers have related the erosion of bare clay surfaces to the excess shear stress, the amount by which the applied bottom shear stress exceeds the critical shear stress (τ_c) for erosion (Parthenaides, 1965; Sheng and Lick, 1979; Amos et al., 1992). The excess shear is used, in a modified form, in the present model:

$$E_{ss} = N_o K_{ss}(\tau{-}\tau_c)^p \tag{18}$$

where E_{ss} is the erosion (m yr^{-1}) by a single wave type at a single tidal level and N_o is the number of waves of that type at that tidal level each year (based on tidal duration, wave period and wave frequency). K_{ss}

and p are calibration coefficients to convert excess shear into erosional units. Zeman's (1986) data suggest that in northern Lake Erie, the relationship between clay erosion and excess shear stresses is essentially linear (p=1), which is similar to Amos et al's. (1992) conclusion that a value of p=0.81 best describes the erosion of fine-grained sediments in the Bay of Fundy. The critical shear stress is a function of the shear strength of the clay as well as its clay content, structure, and other properties (Kamphuis and Hall, 1983). Critical shear stresses for cohesive clays in the southern Great Lakes range from about 0.53 Pa to more than 20 Pa (Coakley et al., 1986; Zeman, 1986; Kamphuis, 1990; Bishop et al. 1992).

An important consideration in calculating rates of abrasion under a beach deposit is the role of sediment thickness. Long-term abrasion rates decrease with beach thickness (Robinson, 1977a), but this is partly because sediment can be moved less frequently under thicker than under thinner deposits. Whether, for a given wave, abrasion is more effective under a thin mobile layer of sediment than under a thick mobile layer, remains to be determined. In a deposit which is almost as thick as the maximum depth of the movable sediment layer, the weight of the sediment may facilitate abrasion and ensure that the abrasives remain in contact with the clay. Conversely, the sediment at the base of a deposit that is much thinner than the maximum thickness of moving sediment, can be swept back and fore over a much higher proportion of the wave period than under thicker deposits, which may only be mobile for a short time under the wave crests. As it is generally assumed that the degree of agitation of the abrasives at the bottom of a beach deposit is more important that the downward pressure exerted on them (Robinson, 1977b; Sunamura, 1992; Blanco-Chao et al., 2007), the expression used to calculate abrasion on a clay surface is based on the ratio of actual sediment thickness to the maximum thickness that can be moved by a given wave at that location:

$$E_a = N_o K_a(\zeta_{t\max}/\zeta_t) \tag{19}$$

where E_a is the abrasion (m yr^{-1}) accomplished by a single wave type operating at a single tidal level, and K_a is a coefficient to convert the sediment thickness ratio into abrasional units. To avoid extremely high computed rates of erosion associated with very large $\zeta_{t\max}/\zeta_t$ values, the minimum thickness for a beach deposit was set at 0.01 m. A simple modification of Eq. (19) could be made to investigate the effect of abrasion rates that increase with the depth of the mobile sediment layer, or are independent of the thickness of the mobile layer.

Wave induced bottom shear stresses and abrasion operate on the clay platform below the water surface, but retreat of the steeply sloping bluffs is accomplished by mechanical wave erosion of *in situ* clay, especially during storms, and the erosion and removal of weathered material fallen or washed down the bluff face. Mechanical wave erosion can also erode exposed surfaces in the intertidal zone (Trenhaile, 2000, 2001, 2005). Erosion is the result of the stresses generated at, or close to, the water surface by the impact of broken waves, and it is represented in the model by Trenhaile's (2000) excess surf stress expression:

$$E_{bf} = N_o K_{bf}(S_F - S_{Fcr}) \tag{20}$$

where: E_{bf} is the recession (m yr^{-1}) accomplished by a single wave type at a single elevation each year, K_{bf} is a wave erosion calibration coefficient that converts surf stress to the rate of bluff or platform recession, S_F is the stress exerted by the surf at the bluff foot (kg m^{-2}), and S_{Fcr} is the threshold, or minimum surf stress, to initiate erosion by wave impact. The surf stress (S_F) is calculated in the model using (Trenhaile, 2000):

$$S_F = \left[0.5\gamma(H_b/0.78)e^{-\chi S_w}\right]\sin^2\varphi \tag{21}$$

where: γ is the specific weight of water (about 9800 kg m^{-3} for fresh water and 1025 kg m^{-3} for seawater), χ is a dimensionless surf attenuation constant, representing the roughness of the bottom, S_w is the width of the surf zone, and φ is the gradient of the clay platform or bluff face at the required tidal level. As in previous studies, a value of χ=0.01 is used to represent smooth-bottomed surf zones, which are typical of clay and other weak rock foreshores (Trenhaile, 2000, 2001). The term $\sin^2\varphi$ represents the reduction in the stress generated by a broken wave on a sloping surface relative to the stress generated by the same wave on a vertical surface (CERC, 1977); therefore, whereas wave impact stresses are important on the bluff and on other steeply sloping surfaces, stresses are generally very low in the gently sloping intertidal zones of clay coasts.

Eqs. (20) and (21) are consistent with the negative feedback relationship that exists between submarine erosion and retreat of the bluff. Slow rates of submarine erosion, relative to rates of bluff retreat, cause the width of the surf zone to increase as the waves break further from the retreating foot of the bluff resulting, through Eq. (21), in lower rates of bluff recession. Conversely, rapid rates of submarine erosion, relative to rates of bluff retreat, reduce the width of the surf zone, resulting in more rapid rates of bluff erosion.

2.5. Model structure and sample runs

The model grid consists of 1500 horizontal levels, 0.1 m apart. Extreme low tide is set at level 850, thereby allowing even very long waves to approach the coast from deep water (Fig. 5), although its elevation can be changed, as required, to examine the effect of rising or falling sea or lake level. The extreme high tide is at level 800+ (T_r/0.1), where T_r is the maximum tidal range, the difference in elevation between the highest, high and lowest, low tidal levels. Model runs require inputted values for the gradient of the initial clay profile, which may be linear or curved, the amount and grain size of any beach material, the tidal range, the critical shear stress of the clay, (τ_c), and the threshold surf stress for erosion by wave impact (S_{Fcr}). Calculating the surf stresses generated by the wave regime used in the sample model runs (Table 1) suggested that a threshold surf stress of 500 kg m^{-2} is suitable to represent more resistant materials that are only eroded by the larger waves in the wave set, and 50 kg m^{-2} for less resistant materials that are eroded by most of the waves in the wave set. These calculations also indicated that a conversion coefficient (K_{bf}) value of 1×10^{-6} provides bluff erosion rates of between about 2.25 and 0.25 m yr^{-1}, which are consistent with rates reported from the

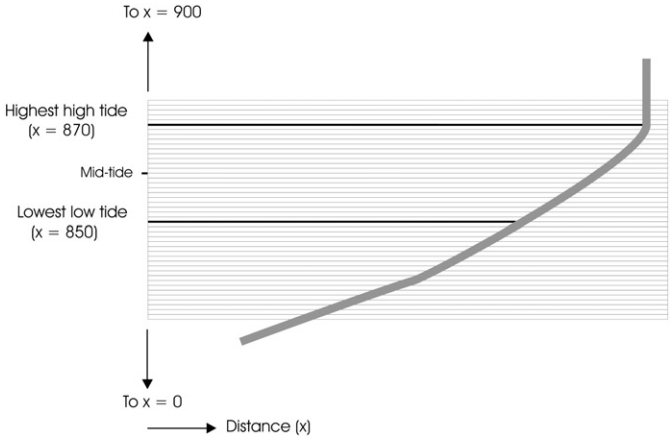

Fig. 5. Model structure for a 2 m tidal range. As the tide occupies each level sequentially between the lowest, low and the highest, high tidal levels, the model calculates erosion by shear stresses and abrasion at 0.1 m vertical intervals from the tidal level down to the deepest level affected by the waves.

Table 1
Wave data used in sample runs (derived from Carvalho, 2003)

H_o (m)	1	2	3	4	5	7	8
T (s)	4.12	5.24	6.19	6.92	7.61	8.69	9.65
% Frequency	9.28	19.13	14.10	8.64	5.98	2.49	0.76

Frequencies are for the percentage of the year in which waves reach west facing coasts in the Azores.

lower Great Lakes and from other clay coasts (Hutchinson, 1973; Kamphuis, 1987).

In the model runs reported here for demonstration purposes, wave data are entered as a series of discrete waves of known deep water height, period, and frequency. Because of the use of annual wave distributions, changes to the profile are made at the end of each year, based on the total amount of bluff recession, and on erosion totals by wave impact stresses, abrasion and bottom shear stresses at each elevation. Changes to the profile from one year to the next are fairly small, and the effect of the lag in the feedback between profile morphology and process is minor. Nevertheless, if the wave data were inputted as time series, changes to the profile would be essentially instantaneous in response to the erosion accomplished by each wave, with no lag between morphology and process. Conversely, the use of time series would make it more difficult to isolate and assess the effect of particular wave types on profile development.

The amount of erosion accomplished below the water surface by shear stresses and abrasion, and at the water surface by abrasion and wave impact stresses, is calculated with the tide at the extreme low tidal level; this procedure is then repeated at each level as the tide rises, in 0.1 m vertical increments, from the low to the high tidal level. The amount of erosion per year at a specific sub- or intertidal elevation is the total accomplished by all the waves when the water surface is at each tidal level, multiplied by the annual number of waves of each type that operate when the tide is at each tidal level (N_o values in Eqs. (18)–(20)).

The model will be used to study the effect of various factors, including changes in lake and sea level, on clay coast erosion and development. Although the present paper is concerned with the structure and derivation of the model, a few runs were made for the equivalent of one year only, to illustrate model mechanics and the type of data that are produced. The runs were made using deep water wave heights, periods, and frequencies derived from hindcast data from a

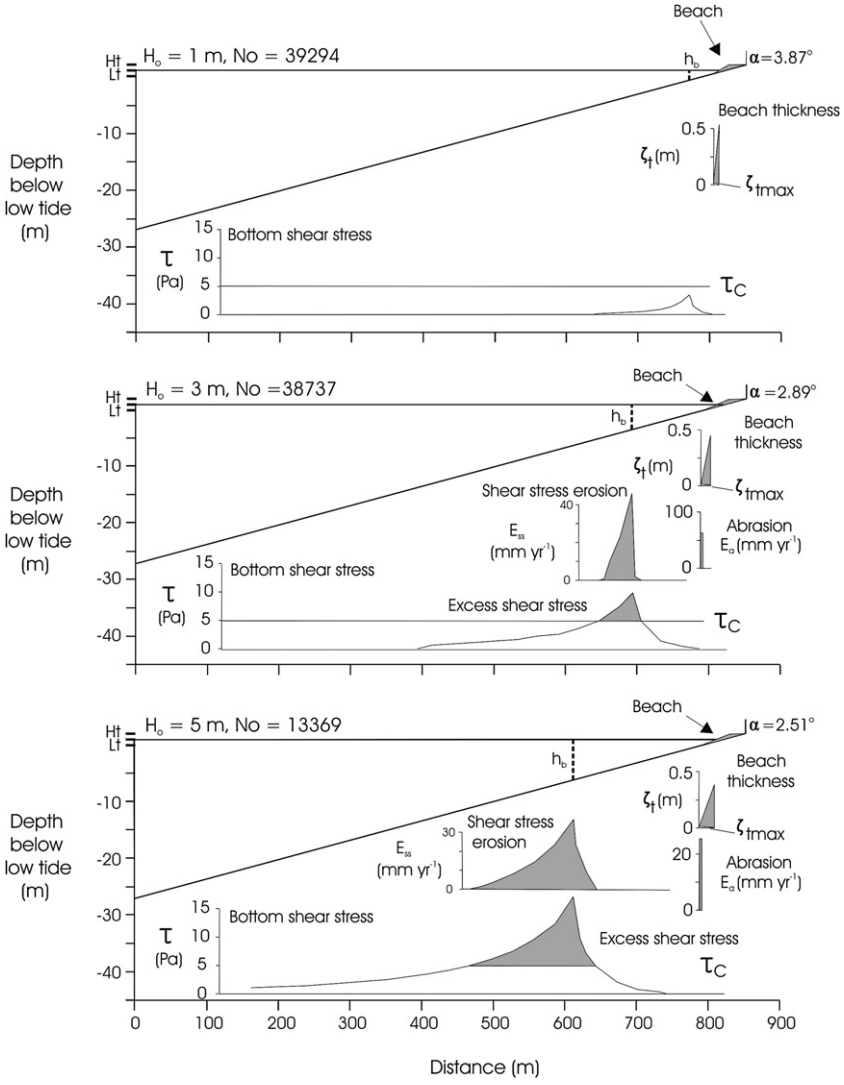

Fig. 6. Example of model runs for deep water waves of 1, 3 and 5 m height at the mid-tidal level after 1 year. The figure shows bottom shear stress, excess shear stress, beachface gradient, and erosion, perpendicular to the surface, by shear stresses and abrasion, for each wave. Beach thickness is shown only for the area extending from the seaward edge of the beach up to the water surface (mid-tide). Data are plotted in the horizontal plane directly below the corresponding location on the profile. There was no wave erosion in the intertidal zone owing to the protection afforded by the beach.

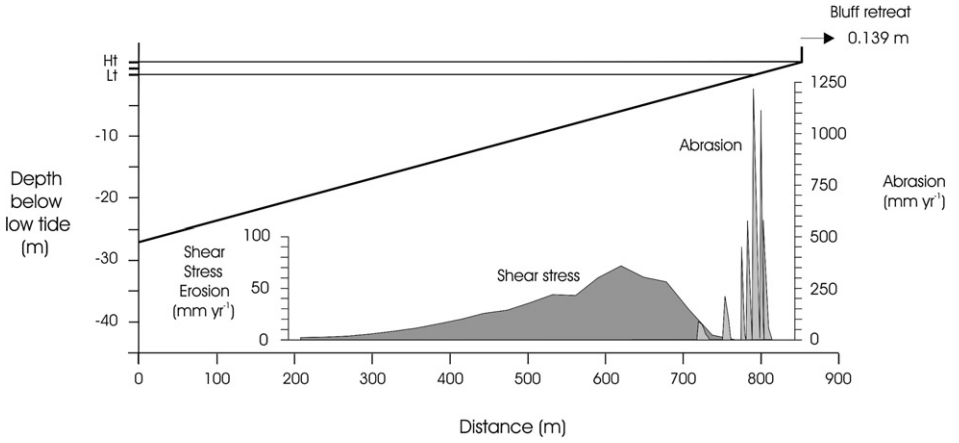

Fig. 7. The annual erosional sum of all seven waves operating at each tidal level (with a frequency determined by N_o in Eqs. (18) and (19)) over a complete tidal cycle. The same values were used for model constants and variables as in Fig. 6. Data are plotted in the horizontal plane directly below the corresponding location on the profile. Bluff retreat is shown for $K_{bf}=1\times10^{-7}$ and $S_{Fcr}=300$ kg m^{-2}.

third generation open sea wind–wave model for the western section of the Atlantic Azores Archipelago (Carvalho, 2003)(Table 1). The tidal range in the runs was 2 m and the corresponding tidal duration values at each 0.1 m elevation were derived from the tidal records from Gaspé, Québec using Smart and Hale's program (1987) (Fig. 3). To eliminate the effect of variable bottom slope on the erosional processes in these preliminary runs, the initial surface was linear with a gradient of 2°. The runs had 20 m^2 of beach material with a grain diameter of 0.001 m. The critical bottom shear stress for erosion in these runs was 5 Pa, which falls within the lower to mid-range of the values obtained from the southern Great Lakes (Coakley et al., 1986; Zeman, 1986; Kamphuis, 1990; Bishop et al. 1992). The conversion constants for shear stress erosion, K_{ss}, and abrasion, K_a, were 2.4×10^{-7} and 1×10^{-6}, respectively. The exponent value p=1 (Eq. (18)) was used to describe the relationship between bottom erosion and excess shear stress. The beach covered the entire intertidal zone and there was no wave erosion in these runs except at the foot of the bluff at the high tidal level.

Profile erosion is shown for a small portion of an annual model run, for the waves with 1, 3, and 5 m deep water heights (Table 1), and with the water surface (tidal level) at mid-tide, where the tidal duration value is 472.5 h yr^{-1} (Fig. 6). Bottom shear stresses increased with wave height, and were greatest under the breakers. The stresses generated by the lowest wave (H_o=1 m) were below the critical value and were unable to erode the clay bottom. Shear stresses generated by the other two waves eroded the profile around the breaker zone, which was located increasingly offshore with increasing wave height. Excess shear stresses increased with increasing wave height, but because of the much higher frequency (N_o in Eq. (18)) of the lower waves at the mid-tidal level, the maximum amount of erosion by shear stresses was higher for the 3 m than for the 5 m high waves. Conversely, excess shear stresses, and therefore erosion, were generated over about 180 m of the bottom around the breaker zone by the 5 m wave, compared with only about 60 m of the bottom by the 3 m wave.

There was not enough sediment in these runs to allow the beach to extend out to the breaker zone where bottom orbital velocities are highest, and the thickness of the mobile sediment layer was generally less than 20 mm. Abrasion occurred only under the 3 m and 5 m waves. Beach thicknesses rapidly increased shorewards, even under the gentler beachfaces of the highest waves, and abrasion was generally limited in these runs to a zone of mobile sediment, about 3–6 m wide, extending landwards from the toe of the beach.

The total annual amount of downwearing accomplished at each elevation by the seven waves in the wave set (Table 1) was distributed in a roughly bimodal pattern (Fig. 7). Erosion by excess shear stresses occurred over a wide area, essentially corresponding to the coalesced near-breaker zones of each wave. Maximum erosion was accomplished under the breaker zones of waves of moderate height (H_o=3 to 5 m), which were often powerful enough, depending on the tidal level, to generate excess shear stresses on the bottom, and much more frequent (N_o values in Eq. (18)) than the higher, more powerful waves in the set which produced progressively lower amounts of erosion in deeper water. In part because of the K_{ss} and K_a values used in these runs, rates of abrasion in the first year were much higher than rates of erosion owing to bottom shear stresses. Abrasion only occurred over a small area associated with the migrating seaward edge of the beach, where the deposits were thin enough to be agitated by the waves. Abrasion rates varied considerably within this zone, reflecting the tendency for the beach edge to occur at specific elevations according to the prevailing wave; negative feedback reduces these effects in model runs over longer periods, as thicker, immobile deposits accumulate in, and subsequently protect, depressions formed by previously rapid abrasion. The total amount of backwearing at the foot of the bluff was 0.139 m in these runs, which used S_{Fcr}=300 kg m^{-2} (Eq. (20)), representing bluff and platform material with a fairly high wave erosional threshold. The lowest waves were too weak and the largest waves were too attenuated to erode the bluff, and all erosion in the first year was attributable to waves with deep water heights of between 2 and 5 m.

Several additional model runs, using the same values for K_{ss}, K_a, and p as previously, were made for periods ranging up to 3000 yr, the time that the sea is generally considered to have reached approximately its present level in the northern hemisphere (Fig. 8). The model quickly developed profiles that were subsequently retained through time as they retreated landwards, although the base of the profiles, at depths at which there was little to no bottom wave orbital motion, became progressively gentler, suggesting that an essentially horizontal basal surface would develop at these depths (Fig. 8, Tables 2–5).The simulated profiles were concave in the upper part of the submarine zone, which reflects the occurrence of maximum shear stresses in the breaker and inner surf zones of the seven wave types. The profiles became more convex at greater depths with the progressive decrease in bottom shear stresses and correspondingly greater preservation of the original profile. The intertidal zone experienced erosion by bottom shear stresses, abrasion, and wave impact stresses, and was generally a gently sloping, essentially linear surface.

Runs 1 and 2 had no sediment and were identical apart from the critical shear stress for erosion and the threshold surf stress to initiate erosion by wave impact. Although the clay was less resistant to

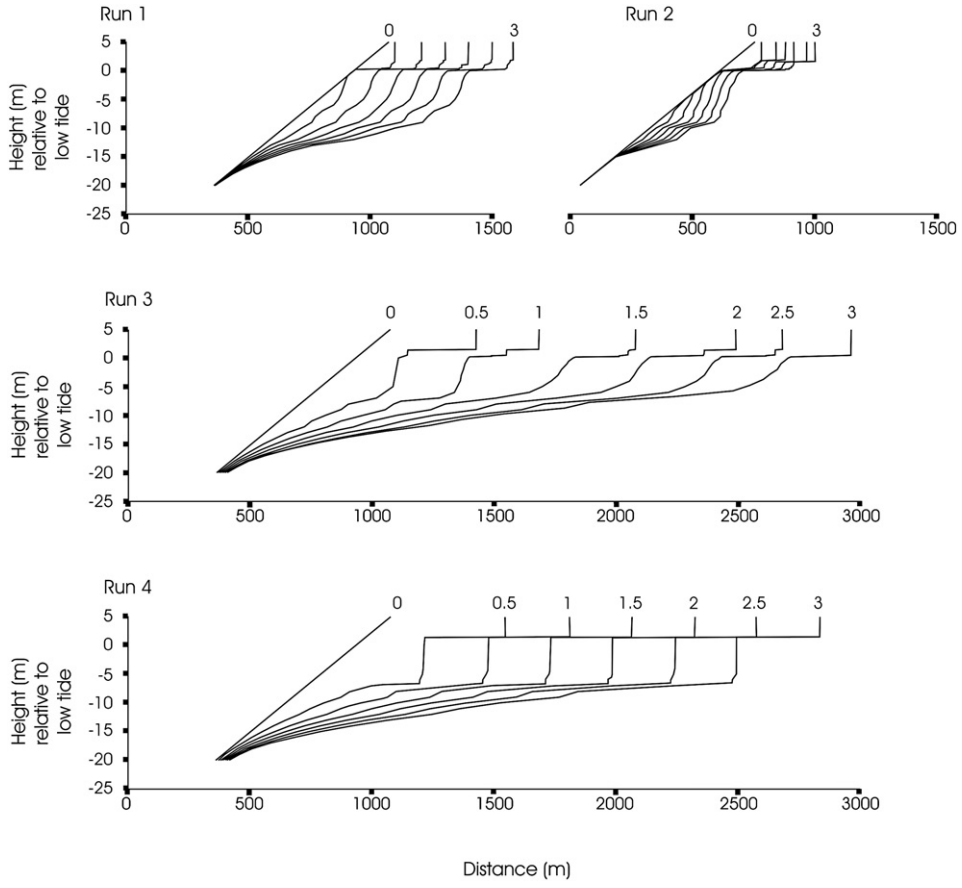

Fig. 8. Examples of model runs over a 3000 yr period. All four runs started with a linear surface with a 2° gradient and a 2 m tidal range. The shear stress, abrasion, and wave erosion calibration coefficients were $K_{ss}=2.4\times10^{-7}$ (Eq. (18)), $K_a=1\times10^{-6}$ (Eq. (19)), and $K_{bf}=1\times10^{-7}$ (Eq. (20)), respectively. There was no sediment in runs 1 and 2, 20 m^2 in run 3, and 60 m^2 in run 40; sediment grain diameter (D) was 1 mm. Run 1 had a critical shear stress for erosion (τ_c) of 10 Pa and a threshold surf stress, to initiate erosion by wave impact (S_{Fcr}) of 300 kg m^{-2}; the corresponding values for Run 2 were 15 and 200. Runs 3 and 4 had a critical shear stress value of 5 Pa, and a threshold surf stress value of 50 kg m^{-2}.

erosion by wave impact in run 2 than in run 1 (S_{Fcr}=200 and 300 kgm^{-2}, respectively), it was less resistant to bottom shear stresses in run 1 than in run 2 (τ_c=10 and 15 Pa, respectively). The occurrence of more rapid bluff erosion in run 1 than in run 2 therefore provided support for the contention that the rate of submarine erosion controls the rate of bluff retreat (Flemming, 1965; Philpott, 1984; Bishop et al.,

Table 2
Mean rates of erosion (m yr^{-1}) through time for run 1

Years						
Depth (m)	0–500	500–1000	1000–1500	1500–2000	2000–2500	2500–3000
2	0.21	0.22	0.20	0.19	0.19	0.18
1	0.25	0.21	0.19	0.19	0.19	0.18
0	0.00	0.00	0.39	0.19	0.19	0.18
−1	0.01	0.22	0.19	0.19	0.19	0.18
−2	0.04	0.22	0.19	0.19	0.19	0.18
−3	0.08	0.22	0.19	0.19	0.19	0.18
−4	0.12	0.22	0.19	0.19	0.19	0.18
−5	0.16	0.21	0.19	0.19	0.19	0.18
−6	0.18	0.20	0.19	0.19	0.18	0.18
−7	0.15	0.19	0.19	0.18	0.18	0.18
−8	0.15	0.20	0.19	0.18	0.18	0.18
−9	0.18	0.19	0.18	0.18	0.18	0.17
−10	0.15	0.16	0.15	0.15	0.15	0.15
−11	0.13	0.14	0.14	0.13	0.13	0.13
−12	0.11	0.12	0.12	0.11	0.11	0.11
−13	0.06	0.07	0.07	0.07	0.07	0.07
−14	0.04	0.05	0.05	0.05	0.05	0.05
−15	0.03	0.03	0.03	0.03	0.03	0.03
−16	0.02	0.02	0.02	0.02	0.02	0.02
−17	0.01	0.01	0.01	0.01	0.01	0.01
−18	0.00	0.00	0.00	0.00	0.00	0.00
−19	0.00	0.00	0.00	0.00	0.00	0.00
−20	0.00	0.00	0.00	0.00	0.00	0.00

Table 3
Mean rates of erosion (m yr^{-1}) through time for run 2

Years						
Depth (m)	0–500	500–1000	1000–1500	1500–2000	2000–2500	2500–3000
2	0.22	0.12	0.08	0.08	0.10	0.07
1	0.23	0.01	0.07	0.08	0.07	0.07
0	0.00	0.00	0.00	0.04	0.07	0.07
−1	0.00	0.00	0.00	0.05	0.07	0.07
−2	0.00	0.00	0.00	0.08	0.07	0.07
−3	0.00	0.00	0.04	0.08	0.07	0.07
−4	0.00	0.00	0.07	0.08	0.07	0.07
−5	0.00	0.04	0.08	0.08	0.07	0.07
−6	0.02	0.07	0.08	0.08	0.07	0.07
−7	0.03	0.08	0.08	0.08	0.07	0.07
−8	0.07	0.09	0.08	0.08	0.07	0.07
−9	0.09	0.08	0.08	0.08	0.07	0.07
−10	0.05	0.06	0.06	0.06	0.06	0.05
−11	0.05	0.06	0.06	0.06	0.05	0.05
−12	0.06	0.06	0.06	0.06	0.05	0.05
−13	0.03	0.03	0.03	0.03	0.03	0.03
−14	0.02	0.02	0.02	0.02	0.02	0.02
−15	0.00	0.00	0.00	0.00	0.00	0.00
−16	0.00	0.00	0.00	0.00	0.00	0.00
−17	0.00	0.00	0.00	0.00	0.00	0.00
−18	0.00	0.00	0.00	0.00	0.00	0.00
−19	0.00	0.00	0.00	0.00	0.00	0.00
−20	0.00	0.00	0.00	0.00	0.00	0.00

Table 4
Mean rates of erosion (m yr^{-1}) through time for run 3

Years						
Depth (m)	0–500	500–1000	1000–1500	1500–2000	2000–2500	2500–3000
2	0.88	0.52	0.78	0.62	0.58	0.56
1	0.36	0.81	1.00	0.62	0.58	0.56
0	0.35	0.57	0.86	0.62	0.58	0.56
−1	0.40	0.55	0.83	0.62	0.58	0.56
−2	0.45	0.54	0.81	0.62	0.58	0.56
−3	0.50	0.53	0.79	0.62	0.58	0.56
−4	0.55	0.53	0.76	0.61	0.58	0.56
−5	0.58	0.53	0.70	0.60	0.57	0.56
−6	0.62	0.52	0.63	0.58	0.56	0.55
−7	0.57	0.49	0.49	0.49	0.49	0.49
−8	0.40	0.37	0.43	0.41	0.40	0.39
−9	0.40	0.35	0.38	0.37	0.37	0.37
−10	0.32	0.28	0.31	0.30	0.30	0.30
−11	0.26	0.24	0.26	0.26	0.25	0.25
−12	0.23	0.21	0.22	0.22	0.22	0.22
−13	0.18	0.17	0.17	0.17	0.17	0.17
−14	0.14	0.13	0.13	0.13	0.13	0.13
−15	0.10	0.09	0.09	0.09	0.09	0.09
−16	0.07	0.07	0.07	0.07	0.07	0.07
−17	0.05	0.05	0.05	0.05	0.05	0.05
−18	0.03	0.03	0.03	0.03	0.03	0.03
−19	0.02	0.02	0.02	0.02	0.02	0.02
−20	0.02	0.02	0.02	0.02	0.02	0.02

1992). Conversely, in runs 5 and 6, which were otherwise identical and had no beach sediment, the occurrence of clays in run 5 that were less resistant to erosion by wave impact stresses than in run 6, resulted in faster erosion by bottom shear stresses through time, at depths up to about 5 m below extreme low tide (Table 6). Although erosion rates converged through time in the two runs and were almost identical after 3000 years, the total amount of erosion accomplished by shear stresses in run 6 was 53 m higher than in run 5 at a depth of 1 m below the low tidal level, and 5.6 m higher at a depth of 5 m below the low tidal level. These runs suggest that rates of bluff retreat by wave impact stresses influence rates of submarine erosion by bottom shear stresses. This reflects the role of bluff recession in determining the rate at which the breaker and inner surf zones, which experience the highest bottom shear stresses, migrate shorewards.

Table 5
Mean rates of erosion (m yr^{-1}) through time for run 4

Years						
Depth (m)	0–500	500–1000	1000–1500	1500–2000	2000–2500	2500–3000
2	1.12	0.52	0.51	0.51	0.51	0.51
1	0.52	0.51	0.51	0.51	0.51	0.51
0	0.57	0.51	0.51	0.51	0.51	0.51
−1	0.63	0.51	0.51	0.51	0.51	0.51
−2	0.68	0.51	0.51	0.51	0.51	0.51
−3	0.74	0.51	0.51	0.51	0.51	0.51
−4	0.80	0.51	0.51	0.51	0.51	0.51
−5	0.84	0.51	0.51	0.51	0.51	0.51
−6	0.88	0.51	0.51	0.51	0.51	0.51
−7	0.53	0.50	0.49	0.49	0.49	0.49
−8	0.42	0.37	0.37	0.37	0.37	0.37
−9	0.41	0.36	0.36	0.35	0.35	0.35
−10	0.32	0.29	0.29	0.29	0.29	0.29
−11	0.27	0.24	0.24	0.24	0.24	0.24
−12	0.23	0.22	0.21	0.21	0.21	0.21
−13	0.18	0.17	0.17	0.17	0.17	0.17
−14	0.14	0.13	0.13	0.13	0.13	0.13
−15	0.10	0.09	0.09	0.09	0.09	0.09
−16	0.07	0.07	0.07	0.07	0.07	0.07
−17	0.05	0.05	0.05	0.05	0.05	0.05
−18	0.03	0.03	0.03	0.03	0.03	0.03
−19	0.02	0.02	0.02	0.02	0.02	0.02
−20	0.02	0.02	0.02	0.02	0.02	0.02

3. Discussion

Given the present state of knowledge on cohesive coastal processes and rates of erosion, particularly in tidal, marine environments, all models, including the present one, have to make a number of assumptions, and they use empirical and theoretical equations, generally involving unknown coefficients that have not been tested in the field. Few surveyed clay coast profile data are available to determine coefficient values under different conditions or to test model validity, especially from tidal environments. Furthermore, the lower portions of some profiles may retain vestiges of former sea levels, with a morphology that is not related to contemporary morphogenic conditions. Nevertheless, although it is not the purpose of this model to replicate specific coastal profiles, model profiles were compared with a few published profiles from Lake Ontario, in southern Canada. The profiles were quite similar in some cases, despite the fact that model profiles from a very exposed wave environment with a 2 m tidal range and a historically constant sea level were compared with profiles from a non-tidal lake with a much less vigorous wave environment (Fig. 9). The ability to replicate the concavity and other gross aspects of the morphology of clay profiles in the field (Coakley et al., 1986; Davidson-Arnott, 1986; Healy et al. 1987; Kamphuis, 1987; Bishop et al. 1992; Walkden and Hall, 2005) suggests that basic model assumptions are correct, but it does not, necessarily, validate the value of the calibration coefficients used in those runs.

Model coefficients can be calibrated by replicating the present morphology of a coast, but 'tuning' a model to produce contemporary morphology does not, necessarily, mean that the selected coefficient values are correct, or that the model would successfully replicate stages in the development of that coast in the past, or would be able to do so in the future. Consequently, it is questionable at present whether models can be used for engineering purposes to simulate the long-term development of a specific cohesive clay coast, or to predict the short-term response of a particular coast to human or natural forces. Conversely, models can be used to investigate the general nature of the relationships that exist between the many factors that influence the erosion and development of clay coasts, and to identify, or emphasize, those poorly understood aspects of clay coast morphodynamics that hinder our ability to forecast their development and probable response to a variety of natural and anthropogenic forcing factors.

Preliminary model runs suggest that bluff, intertidal, and subtidal erosion rates on clay coasts are interdependent and that the relationships between them are more complex than was previously believed.

Table 6
Mean rates of erosion (m yr^{-1}) through time for runs 5 and 6

Depth (m)	Years							
	Run 5				Run 6			
	0–500	500–1000	1000–2000	2000–3000	0–500	500–1000	1000–2000	2000–3000
2	0.51	0.09	0.08	0.07	0.03	0.09	0.08	0.07
1	0.52	0.10	0.08	0.07	0	0.16	0.07	0.07
0	0.03	0.09	0.08	0.07	0	0	0.07	0.07
−1	0.03	0.08	0.08	0.07	0	0.02	0.07	0.07
−2	0.04	0.09	0.08	0.07	0.01	0.05	0.07	0.07
−3	0.06	0.09	0.08	0.07	0.04	0.06	0.07	0.07
−3	0.08	0.09	0.08	0.07	0.06	0.07	0.07	0.07
−5	0.07	0.08	0.08	0.07	0.07	0.07	0.07	0.07
−6	0.07	0.07	0.07	0.07	0.08	0.07	0.07	0.07
−7	0.06	0.06	0.06	0.06	0.06	0.06	0.06	0.06
−8	0.05	0.05	0.05	0.04	0.05	0.05	0.05	0.05
−9	0.04	0.04	0.04	0.04	0.05	0.04	0.05	0.05

There was no sediment in either run. The initial slope gradient was 2° and the tidal range was 2 m. K_{ss} was $2.4\times10^{-8}$and K_{bf} was 1×10^{-7}. τ_c was 5 Pa in both runs and S_{Fcr} was 50 and 500 kg m^{-2} in runs 5 and 6, respectively.

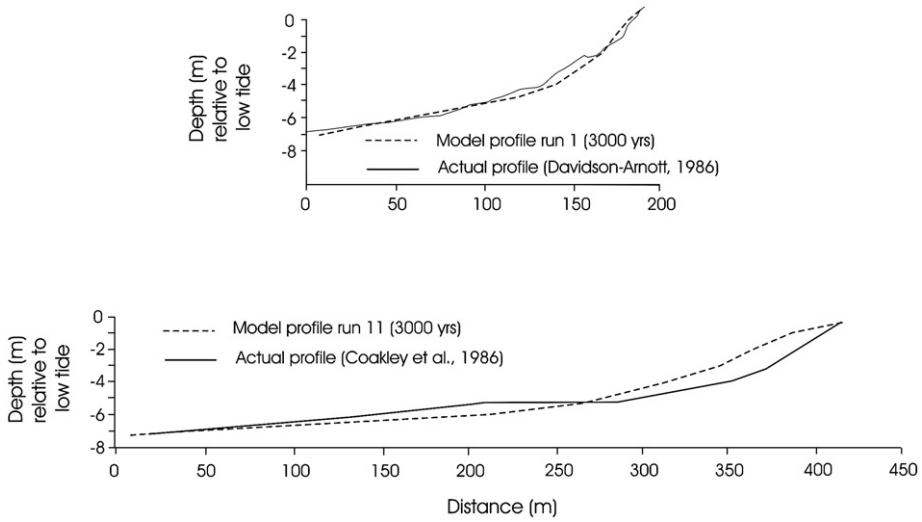

Fig. 9. Comparisons between model (after 3000 years) and clay profiles from Lake Ontario, Canada. Profile 11 had a 2° initial slope, a tidal range of 2 m, and 20 m^2 of 0.001 m diameter sand. τ_c was 5 Pa and S_{Fcr} was 50 kg m^{-2}. K_{ss}, K_a, and K_{bf} were 2.4.10^{-7}, 1×10^{-6}, and $1\times10–10^{-7}$, respectively. The specifications for run 1 are described in the text.

Whereas rates of submarine erosion affect rates of bluff and platform erosion, rates of bluff and platform erosion also appear to exert control over rates of submarine erosion. This is supported by theoretical considerations, based on the relationship between bottom gradients and depths and rates of wave attenuation, breaker depths, and surf zone widths. The intertidal and subtidal zones of equilibrium profiles, that retain their general shape as they migrate landwards ((Philpott, 1984; Davidson-Arnott, 1986; Bishop et al. 1992), must be wider and more gently sloping in clays that are more susceptible to erosion by wave impact stresses than in clays that are less susceptible. This is because the degree of wave attenuation needed to reduce rates of wave erosion of the bluff and platform to that of shear stress erosion rates on the bottom is related to the susceptibility of the clay to wave impact; consequently, the more susceptible the clay, the greater the wave attenuation that is required, and the gentler and wider the profile that must develop. Bluff retreat may also influence rates of intertidal and subtidal abrasion, because as a bluff retreats, beach deposits move landwards and, unless there is a commensurate increase in sediment supply and in the ability of the foreshore to retain it, the narrow abrasion zone at the foot of the beach must also migrate landwards (Blanco-Chao et al., 2007). Nevertheless, although these preliminary runs suggests that there are complex interrelationships between subtidal, intertidal, and bluff erosion rates and processes, many more runs must be made to determine their nature and occurrence under different geological, tidal, and wave conditions.

4. Conclusions

The model discussed in this paper was developed to examine relationships between variables that affect the erosion and development of cohesive clay coasts. The model considers the effect of wave induced shear stresses on the bottom, wave impact stresses at the water surface on the bluff and intertidal platform, and abrasion at and below the water surface near the thin, seaward edge of the beach. The model shares some of the characteristics of previous cohesive coast models, including the assumptions that bottom shear stresses are primarily responsible for the erosion of bare clay surfaces and abrasion for surfaces under mobile sheets of sand or gravel. It differs from previous models in several important ways, including: the prediction of beach occurrence and morphology; estimates of mobile beach depth; consideration of the effect of ripple occurrence and morphology on wave friction factors and beach mobility; the calculation and use of tidal duration values; and the incorporation of wave erosion at the water surface in the intertidal zone and at the foot of clay bluffs. The model produces concave submarine profiles that are similar to those in the field and is able to replicate the morphology of clay coast profiles in the Great Lakes. The model also produces equilibrium profiles that experience the same rate of erosion from the foot of the bluff to 6 to 8 m below the extreme low tidal level.

Notation

A_b	half the length of the horizontal water motion at the bottom
C	wave celerity (speed) in intermediate and shallow water
Cn	group wave celerity
C_o	deep water wave celerity
D	beach sediment grain diameter
D_b	distance shorewards from the breakers
E	wave energy
E_a	annual erosion by abrasion by a single wave type at a single tidal level
E_{bf}	amount of bluff recession per year
E_{ss}	annual erosion by bottom shear stresses by a single wave type at a single tidal level
F_w	wave friction factor
g	acceleration due to gravity
H	wave height in intermediate/shallow water
H_b	mean breaker height.
H_o	wave height in deep water
h	water depth
h_b	depth of wave breaking
K_a	abrasion calibration coefficient
K_{bf}	wave erosion calibration coefficient
K_{ss}	excess shear stress calibration coefficient
k	the wave number
k_s	Nikuradse roughness length for a rippled bed or the equivalent roughness length for a plane bed.
L	wavelength in intermediate or shallow water
L_o	wavelength in deep water
N_o	number of waves of a particular type at a particular tidal level per year.
p	shear stress exponent
R_η	ripple height
R_λ	ripple wavelength
S_F	surf stress exerted by a particular wave type at the bluff foot

S_{Fcr}	threshold, or minimum surf stress, to initiate bluff erosion by wave impact
S_w	width of the surf zone
T	wave period
T_r	maximum tidal range
u_o	maximum bottom orbital velocity
α	beachface gradient
β	slope of the surf zone
γ	specific weight of water
γ_b	breaker depth index
ζ_t	beach sediment thickness
$\zeta_{t\max}$	maximum thickness of the moving sediment layer
η	mean water surface elevation relative to the still water level
$d\eta/dx$	gradient of the water surface in the surf zone
Θ	Shields Parameter
Θ_b	Shields Parameter at the breakpoint
Θ_{cr}	critical or threshold Shield Parameter for onset of grain movement
ρ	density of sea water
ρ_s	density of beach sediment
τ	bottom shear stress
τ_c	critical clay shear stress for erosion
φ	local gradient of the clay platform surface at an intertidal elevation
χ	surf attenuation constant, representing the roughness of the bottom
ψ	Mobility Number

Acknowledgement

Financial support for this work, through a Discovery Grant (NSERC 205001-2) from the Natural Sciences and Engineering Research Council of Canada, is gratefully acknowledged.

References

Amos, C.L., Daborn, G.R., Christian, H.A., Atkinson, A., Robertson, A., 1992. In situ erosion measurements on fine-grained sediments from the Bay of Fundy. Marine Geology 108, 175–196.

Balsillie, J.H., Tanner, W.F., 2000. Red flags on the beach, part II. Journal of Coastal Research 16, iii–x.

Battjes, J.A., 1974. Surf similarity. Proceedings of the 14th Coastal Engineering Conference, pp. 466–479.

Bishop, C.T., Skafel, M.G., Nairn, R., 1992. Cohesive profile erosion by waves. Proceedings of the 23rd Coastal Engineering Conference, pp. 2976–2989.

Blanco-Chao, R., Perez Alberti, A., Trenhaile, A.S., Costa Casais, A., Valcarcel-Diaz, M., 2007. Shore platform abrasion in a para-periglacial environment, Galicia, north-western Spain. Geomorphology 83, 136–151.

Carvalho, F., 2003. Elementos do Clima de Agitação Marítima no Grupo Central dos Açores. Instituto de Meteorologia, Lisboa.

CEM, 2002. U.S. Army Corps of Engineers. Coastal Engineering Manual. Engineer Manual, 6 volumes. U.S. Army Corps of Engineers, Washington, D.C., pp. 1110–2-1100.

CERC, 1977. Shore Protection Manual. U.S. Army Corps of Engineers, Coastal Engineering Research Center, Washington DC.

Coakley, J.P., Rukavina, N.A., Zeman, A.J., 1986. Wave-induced subaqueous erosion of cohesive tills: preliminary results. In: Skafel, M.G. (Ed.), Proceedings of the Symposium on Cohesive Shores. National Research Council of Canada (ACROSES), Ottawa, pp. 120–136.

Coffey, F.C., Nielsen, P., 1984. Aspects of wave current boundary layer flows. Proceedings of the 19th Coastal Engineering Conference, pp. 2232–2245.

Dalrymple, R.W., Knight, R.J., Zaitlin, B.A., Middleton, G.V., 1990. Dynamics and facies model of a macrotidal sand-bar complex, Cobequid Bay–Salmon River Esturary (Bay of Fundy). Sedimentology 37, 577–612.

Davidson-Arnott, R.G.D., 1986. Rates of erosion of till in the nearshore zone. Earth Surface Processes and Landforms 11, 53–58.

Davidson-Arnott, R.G.D., Langham, D.R.J., 2000. The effects of softening on nearshore erosion of a cohesive shoreline. Marine Geology 166, 145–162.

Davidson-Arnott, R.G.D., Ollerhead, J., 1995. Nearshore erosion on a cohesive shoreline. Marine Geology 122, 349–365.

Diegaard, R., Fredsoe, J., Hedegaard, I.B., 1986. Suspended sediment in the surf zone. Journal of Waterway, Port, Coastal and Ocean Engineering (ASCE) 112, 115–128.

Engelund, F., Hansen, E., 1967. A Monograph on Sediment Transport in Alluvial Streams. Teknisk Forlag, Copenhagen.

Fisheries and Oceans Canada, 2006. Canadian Tide and Current Tables. Ottawa, Canada. Available online at: http://www.waterlevels.gc.ca/english/Canada.shtml.

Flemming, N.C., 1965. Form and relation to present sea level of Pleistocene marine erosion features. Journal of Geology 73, 799–811.

Healy, T., Sneyd, A.D., Werner, F., 1987. First approximation sea-level dependent mathematical model for volume eroded and submarine profile development in a semi-enclosed sea: Kiel Bay, western Baltic. Mathematical Geology 19, 41–56.

Hutchinson, J.N., 1973. The response of London Clay cliffs to differing rates of toe erosion. Geologia Applicata e Idrogeologia 8, 221–239.

Johnson, D.W., 1919. Shore Processes and Shoreline Development. Wiley, New York.

Justensen, P., 1988. Turbulent wave boundary layers. Institute of Hydrodynamics and Hydaraulic Engineering, Technical University of Denmark, Lyngby, Denmark, series paper 43.

Kamphuis, J.W., 1986. Erosion of cohesive bluffs, a model and a formula. In: Skafel, M.G. (Ed.), Proceedings of the Symposium on Cohesive Shores. National Research Council of Canada (ACROSES), Ottawa, pp. 226–245.

Kamphuis, J.W., 1987. Recession rate of glacial till bluffs. Journal of Waterway, Port, Coastal and Ocean Engineering (ASCE) 113, 60–73.

Kamphuis, J.W., 1990. Influence of sand or gravel on the erosion of cohesive sediment. Journal of Hydraulic Research 28, 43–53.

Kamphuis, J.W., Hall, K.R., 1983. Cohesive material erosion by unidirectional current. Journal of the Hydraulics Division (ASCE) 109, 49–61.

Kanyaya, J.I., Trenhaile, A.S., 2005. Tidal wetting and drying on shore platforms: an experimental assessment. Geomorphology 70, 129–146.

Madsen, O.S., Grant, W.D., 1976. Quantitative description of sediment transport by waves. Proceedings of the 15th Coastal Engineering Conference, pp. 1093–1112.

Nairn, R.B., Pinchin, B.M., Philpott, K.L., 1986. Cohesive profile development model. In: Skafel, M.G. (Ed.), Proceedings of the Symposium on Cohesive Shores. National Research Council of Canada (ACROSES), Ottawa, pp. 246–261.

Nielsen, P., 1992. Coastal Bottom Boundary Layers and Sediment Transport. World Scientific, Singapore.

O'Donoghue, T., Doucette, J.S., Van der Werf, J.J., Ribberink, J.S., 2006. The dimensions of sand ripples in full-scale oscillatory flows. Coastal Engineering 53, 997–1012.

Parthenaides, E., 1965. Erosion and deposition of cohesive soils. Journal of the Hydraulics Division (ASCE) 91, 105–139.

Philpott, K.L., 1984. Comparison of cohesive coasts and beach coasts. In: Kamphuis, J.W. (Ed.), Proceedings, Coastal Engineering in Canada. Queen's University, Kingston, Ontario, pp. 227–244.

Robinson, L.A., 1977a. Marine erosive processes at the cliff foot. Marine Geology 23, 257–271.

Robinson, L.A., 1977b. Erosive processes on the shore platform of northeast Yorkshire. Marine Geology 23, 339–361.

Sheng, Y.P., Lick, W., 1979. The transport and resuspension of sediments in a shallow lake. Journal Geophysical Research 84, 1809–1826.

Short, A.D. (Ed.), 1999. Handbook of Beach and Shoreface Morphodynamics. Wiley, New York.

Skafel, M.G., 1995. Laboratory measurement of nearshore velocities and erosion of cohesive sediment (till) shorelines. Coastal Engineering 24, 343–349.

Skafel, M.G., Bishop, C.T., 1994. Flume experiments on the erosion of till shores by waves. Coastal Engineering 23, 329–348.

Sleath, J.F.A., 1984. Sea Bed Mechanics. Wiley, Chichester.

Smart, C.C., Hale, P.B., 1987. Exposure and inundation statistics from published tide tables. Computers and Geosciences 13, 357–368.

Sunamura, T., 1985. A simple relationship for predicting wave height in the surf zone with a uniformly sloping bottom. Transactions of the Japanese Geomorphological Union 6–4, 361–364.

Sunamura, T., 1989. Sandy beach geomorphology elucidated by laboratory modeling. In: Lakhan, V.C., Trenhaile, A.S. (Eds.), Coastal Modeling: Techniques and Applications. Elsevier, Amsterdam, pp. 159–213.

Sunamura, T., 1992. Geomorphology of Rocky Coasts. Wiley, Chichester, UK.

Sunamura, Y., Kraus, N.C., 1985. Prediction of average mixing depth of sediment in the surf zone. Marine Geology 62, 1–12.

Traykovski, P., 1999. Geometry, migration and evolution of wave orbital ripples at LEO-15. Journal of Geophysical Research 104 (C1), 1505–1524.

Trenhaile, A.S., 1987. The Geomorphology of Rock Coasts. Oxford University Press, Oxford, UK.

Trenhaile, A.S., 2000. Modeling the evolution of wave-cut shore platforms. Marine Geology 166, 163–178.

Trenhaile, A.S., 2001. Modeling the Quaternary evolution of shore platforms and erosional continental shelves. Earth Surface Processes and Landforms 26, 1103–1128.

Trenhaile, A.S., 2004. Modeling the accumulation and dynamics of beaches on shore platforms. Marine Geology 206, 55–72.

Trenhaile, A.S., 2005. Modelling the effect of waves, weathering and beach development on shore platform development. Earth Surface Processes and Landforms 30, 613–634.

Trenhaile, A.S., 2006. Tidal wetting sand drying on shore platforms: an experimental study of surface expansion and contraction. Geomorphology 76, 316–331.

Trenhaile, A.S., Porter, N.J., Kanyaya, J.I., 2006. Shore platform processes in eastern Canada. Géographie Physique et Quaternaire 60, 19–30.

Van Rijn, L.C., 1989. Handbook of Sediment Transportation by Currents and Waves. Delft Hydraulic Report H 461. Delft, The Netherlands.

Vincent, C.E., Young, R.A., Swift, D.J.P., 1981. Bed-load transport under waves and currents. Marine Geology 39, M71–M80.

Vongvisessomjai, S., 1984. Oscillatory ripple geometry. Journal of the Hydraulics Division (ASCE) 110, 247–266.

Walkden, M.J.A., Hall, J.W., 2005. A predictive mesoscale model of the erosion and profile development of soft rock shores. Coastal Engineering 52, 535–563.
Watanabe, A., Riho, Y., Horikawa, K., 1980. Beach profiles and on–offshore sediment transport. Proceedings of the 17th Coastal Engineering Conference, pp. 1106–1121.
Wiberg, P.L., Harris, C.K., 1994. Ripple geometry in wave-dominated environments. Journal of Geophysical Research 99 (C4), 775–789.
Williams, J.J., Thorne, P.D., Heathershaw, A.D., 1989. Comparisons between acoustic measurements and predictions of the bedload transport of marine gravels. Sedimentology 36, 973–979.
Wright, L.D., Short, A.D., 1984. Morphodynamic variability of surf zones and beaches: a synthesis. Marine Geology 56, 93–118.
Zeman, A.J., 1986. Erodibility of Lake Erie undisturbed tills. In: Skafel, M.G. (Ed.), Proceedings of the Symposium on Cohesive Shores. National Research Council of Canada (ACROSES), Ottawa, pp. 150–169.